Electro-deposition of Cobalt and Cobalt-Antimony from Non-Aqueous Media Containing Ethylene Glycol

FLORENTINA GOLGOVICI, MARIANA LILI MARES, ANCA COJOCARU*
Faculty of Applied Chemistry and Materials Science, University Politehnica of Bucharest, 132 Calea Grivitei, Bucharest, Romania

Cobalt deposition and cobalt and antimony co-deposition were evidenced in two non-aqueous electrolytes, both with advantage of a larger electrochemical window: one with ethylene glycol as solvent and the other one a choline chloride based ionic liquid with ethylene glycol as the second component of eutectic mixture. Deposition of singular antimony was also studied in both media. Cyclic voltammetry and electrochemical impedance spectroscopy were used under various conditions (scan rate, ion concentration). A single pair of reduction/oxidation processes was evidenced in CV curves for individual deposition. In ionic liquids with both Co and Sb ions, a first process of Sb deposition occurs before Co + Sb co-deposition. Analyzing Nyquist and Bode spectra the differences between impedance behaviour at various cathodic polarization were observed.

Keywords: cobalt, cobalt-antimony compound, electro-deposition, ethylene glycol, choline chloride based ionic liquid

Cobalt attracted a great interest in view of applications in the production of alloys, sensors, heterogeneous catalysts, in energy storage and for magneto-optic recording media. Cobalt is one of the most typical ferromagnet and the microelectronic industry is a consumer of many kinds of magnetic thin films and nanostructures. Antimony as pure metallic (semimetallic) material is not often used in industry. However, its alloys and chemical compounds (semiconductors) have found wide applications in solar cells, humidity sensors and especially for thermoelectrical generators, thermopile sensors and microcoolers [1]. For instance, $CoSb_3$ (cobalt triantimonide) as films or nanowires is a compound with skutterudite type crystal-structure which has used recently in thermoelectric applications [2]. $CoSb_3$, as well as $ZnSb_3$, possesses high carrier mobility, high electrical conductivity and relatively large Seebeck coefficients. The reduced thermal conductivity was confirmed by the measurements of $CoSb_{2.86}M_{0.02}Te_{0.12}$ (M = Ge, Sn), which show that Ge and Sn enter into the Sb-site of $CoSb_3$ and generate significant changes in the vibration modes [3]. Furthermore, nanostructure with fine grains and "nanodots" contributes to the reduction of thermal conductivity. Ballikaya et al. [4] show that Yb atom is also one of the most effective species to fill the voids in the $CoSb_3$ skutterudite structure in order to reduce the thermal conductivity and thus enhance the thermoelectric performances. These authors established that small quantities of Ce with In may be good partner with Yb to reduce the thermal conductivity.

An electrochemical study of cobalt electrodeposition onto a platinum electrode from an aqueous solution containing 10^{-2} M $CoCl_2$ and 1 M NH_4Cl was carried out [5]. The voltammetric data clearly showed that a process of cobalt underpotential deposition (UPD) takes place during the application of potential in the less negative region. Formation of the cobalt adlayer involved the simultaneous presence of both adsorption and 2D nucleation processes. Zaraska et al. [6] successfully prepared antimony by galvanostatic electrodeposition from two electrolytes: one contains $SbCl_3$ (0.02 M) + citric acid (0.1 M) + sodium citrate (0.05 M) and the other contains 1.8 g/L and 7 g/L tartaric acid (in order to have 0.075 M antimonyl potassium tartrate). Bryngelsson et al. [7,8] reported the synthesis of Sb-based nanoscale coatings which were electrodeposited from tartrate solutions.

The literature data about the co-deposition of cobalt and antimony are very scarce. Direct current electrodeposition was used to co-deposit cobalt and antimony in aqueous solutions, especially in citric-based solutions [9,10]. The standard electrode potentials in aqueous solutions are as follows [10]: E^0 (Sb^{3+}/Sb) = +0.212 V and E^0 (Co^{2+}/Co) = -0.277. Thus, antimony is the nobler metal and this fact determines the use of complex forming agents in order to shift the deposition potentials of antimony with cobalt closer. The effects of agitation, temperature and citric acid content in the electrolyte on the composition and appearance of the alloy deposits, as well as the current efficiency of deposition are reported. Growth behaviour of Co–Sb alloy thin films was systematically studied [11,12] under various deposition conditions. Effects of deposition parameters on the microstructure, chemical, and phase composition of the deposited Co-Sb were also studied.

Based on the chemical composition of the deposits, it was established that the most successful electrolytes contained a 10:1 atomic ratio of cobalt(II) to antimony(III) [2].

Many research programmes have been developed to substitute cobalt electrodeposition from aqueous solutions which is accompanied by an intense hydrogen evolution and therefore has not always satisfactory current efficiency. Electrolytic media with organic solvents were tried to be used. Tseung and his coworkers [13] reported Co deposition from N-N dimethylformamide (DMF) and confirmed the suggestion of Grzybkowski and Pilarczyk [14] that the coordinated forms of $CoCl_2$ in DMF medium are $[Co(DMF)_6]^{2+}$, $[CoCl(DMF)_5]^{+}$ and $[CoCl_3DMF]^{-}$ ionic species. The proposed mechanism [13] consisted in a

* *email: a_cojocaru@chim.upb.ro*

reduction with two-electrons single step, with Tafel slope of 62 mV/dec and transfer coefficient of 0.48:

$$[CoCl_3DMF]^- + 2\,e \rightarrow Co + 3\,Cl^- + DMF \quad \text{(rate determining step, rds)} \quad (1)$$

The same authors [15] reported the deposition process of cobalt from cobalt(II) thiocyanate solution in N,N-dimethylformamide (DMF) with the addition of Cl^- ions. In this case, the mechanism of the deposition of cobalt is *via* electron-transfer/mass-transfer control. Chloride ions act as a competitive ligand substitute for SCN^- ions, thus inhibiting the Co deposition. A conclusion [16] is that deposition of cobalt in nonaqueous solutions greatly depends on the nature of metal ion complexes with anions and this effect is much greater than the one in aqueous solutions.

Ionic liquids are promising electrolytes for electrodeposition of various metals, since they have wide working temperature range, wide electrochemical windows and good thermal and chemical stability. The electrodeposition of cobalt was first performed from ionic liquids based on 1-ethyl-3-methylimidazolium chloride (EMIC) [17,18]. Freyland [19] reported Co deposition from ionic liquids based on 1-buthyl-methylimidazolium salts ($AlCl_3$–[BMIM]Cl and $AlCl_3$–[BMIM]PF_6). Ali et al. [20] used a $CoCl_2$-BPC ionic liquid for Co deposition onto Pt. They established that a low concentration of electroactive species $CoCl_3^-$ and a high concentration of inactive species (tetrahedral chlorocomplex) $CoCl_4^{2-}$ exist. The mechanism proposed was:

$$CoCl_x^{(x-2)-} + e \Leftrightarrow CoCl_x^{(x-1)-}(ads) \quad (2)$$
$$CoCl_x^{(x-1)-}(ads) \rightarrow Co^{+}(ads) + x\,Cl^-(ads) \quad (3)$$
$$Co^+(ads) + e \Leftrightarrow Co \quad (4)$$

The Co electrodeposition procedure was used from 1-n-buthyl-1-methylpyrrolidinum bis-trifluoromethyl sulfonyl imide ([BMP]TFSI)[21,22] or amide ([BMP]TFSA) [21]. An, Yang and Su [23-25] have studied the electrodeposition of Co from EMIC room temperature ionic liquid and from a mixture of EMIC with ethylene glycol; they showed that the cobalt coating from these media was uniform, dense, shining in appearance with good adhesion to the platinum substrate. Yang and Sun [26] prepared Sb from EMIM chloride tetrafluoborate. However, electrolytes with imidazolium derivates have expensive costs and potentially toxicological and purity issues. A new generation of ionic liquids uses eutectic mixtures of quaternary ammonium salts (mostly choline chloride, **ChCl**) with amides, glycols or carboxilic acids. In a study on vitreous carbon, Gomez et al. [27] have shown the possibility to choose of electrodepositing potentials for Co films prepared from ChCl-urea. Previously, we reported some results regarding the possibility of electrodeposition of Sb as element from the same eutectic mixture (1:2 mole ratio) of choline chloride with urea as hydrogen bond donor [28,29]. We present in this paper the preliminary results regarding cobalt deposition and cobalt and antimony co-depositing in two non-aqueous solutions: one with ethylene glycol as solvent and the other one a choline chloride based ionic liquid with ethylene glycol as the second component of eutectic mixture (1:2 mole ratio). We mention that a deposition process of CoSb as thermoelectric semiconductor films was investigated in a nonaqueous solution of ethylene glycol at 120^{0}C in a recent paper [30]. From our knowledge the deposition from ionic liquids of cobalt and cobalt-antimony films is reported for the first time in literature.

Experimental part

Choline chloride (ChCl), ethylene glycol (EG), cobalt (II) chloride hexahydrate, $K_2[Sb_2(tartrate)_2]\cdot 3H_2O$ (antimony potassium tartrate trihydrate) and $SbCl_3$ were used as received. The electrolytes at 25^{0}C containing ethylene glycol as solvent were prepared by adding $CoCl_2 \cdot 6H_2O$ or/ and $K_2[Sb_2(tartrate)_2] \cdot 3H_2O$ as precursors for Co(II) and Sb(III) ions. ChCl-EG eutectic ionic liquid (1:2 molar ratio) was obtained by mixing both reagents and heated at 90^{0}C for 30 min with permanent stirring. In this solvent, $CoCl_2 \cdot 6H_2O$ and $SbCl_3$ were then added at 60^{0}C.

A computer driven Zahner elektrik IM6e potentiostat was used in cyclic voltammetry (5-1000 mVs^{-1} scan rates) and electrochemical impedance spectroscopy EIS (10 mV *ac* voltage, 200 kHz – 50 mHz frequency) experiments. The conventional three-electrode cell contains a stationary working electrode as a Pt foil (0.5 cm^2) or disk (3 mm diameter) and a platinum plate as auxiliary electrode. The electrode potentials were measured in EG based solutions against Ag/AgCl reference electrode, while in ChCl-EG ionic liquids an Ag wire was a quasi-reference electrode.

Results and discussions

Studies in solutions with ethylene glycol as solvent

Cyclic voltammetry was first performed in order to identify the electrodeposition processes of cobalt or antimony. Figure 1 shows cyclic voltammograms obtained in solutions of 264 mM $CoCl_2$ and 540 mM $CoCl_2$ with ethylene glycol as solvent. When compared to the voltammogram of the pure EG solvent (not shown here), the presence of the Co(II) ions in solution gives rise to a single pair of reduction and oxidation processes.

On the reduction branch of voltammograms the onset of a first cathodic region attributed to underpotential deposition (UPD) of cobalt is observed at around 0 V potential for both cobalt ion concentrations. This UPD process is a surface-limited reaction of Co atoms deposited on the naked Pt substrate. Then a shoulder in the potential range from -0.25 V up to -1.25, or even -1.5 V, is noticed, with current densities increasing with the scan rate and cobalt ion concentration. This part represents the massive deposition of cobalt as multilayer and may be considered as a mass-transport controlled process. Finally, at very negative potentials the sudden increase of current is certainly due to the involving of other reduction processes which are probable the cathodic reduction of EG solvent molecules together with hydrogen evolution as a result of reduction of water introduced with cobalt chloride hexahydrate.

Regarding the anodic branches of voltammograms, a very distinct anodic peak of Co dissolution and stripping from Pt is observed in the range from +0.5 V to +1.2 V. Obviously, its peak potential and peak current are strongly influenced by the scan rate and cathodic limit where the scan is inversed. A supplementary anodic process which begins at +1.3 V represents the oxidation of some quantities of chloride ions (Cl^-) which may be accompanied with a further oxidation of Co(II) ions to Co(III) ionic species.

Figures 2 show the EIS curves obtained by polarization with two different cathodic potential values, one where the massive deposition of cobalt did not begin (-0.3V) and the other one where a significant deposition takes place (at -1 V). Thus, the impedance results are interpreted in relation with voltammetric results. The Nyquist diagram shows the dependence of imaginary part of impedance vs. real part of impedance in the shape of capacitive semicircles with a drastical decrease of diameter; this means a decrease of charge transfer resistance implying

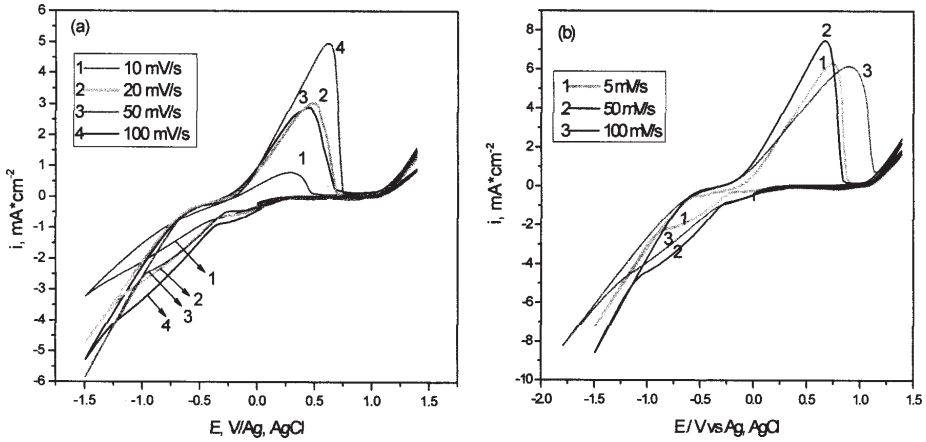

Fig. 1. Cyclic voltammograms on Pt at 25^{0}C for 264 mM $CoCl_2$ (a) and 540 mM $CoCl_2$ (b), dissolved in ethylene glycol at different scan rates

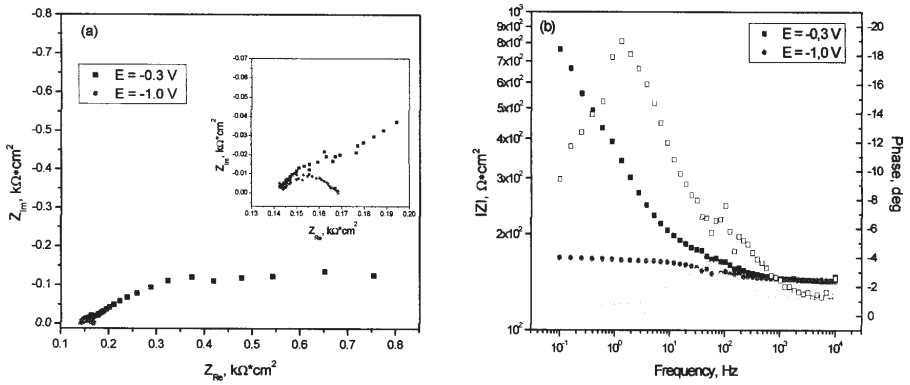

Fig. 2. Nyquist (a) and Bode (b) diagrams on Pt electrode from ethylene glycol + 264 mM $CoCl_2$, 25^{0}C, at various polarization potentials

an intense deposition rate at -1 V compared to -0.3 V. The Bode diagram represents simultaneously two dependences, namely impedance modulus *vs*. frequency and phase angle *vs*. frequency. This diagram shows a decrease of impedance modulus but also a change of negative phase angle from -20^0 to -4^0 proving the significant metallic character of Co deposit.

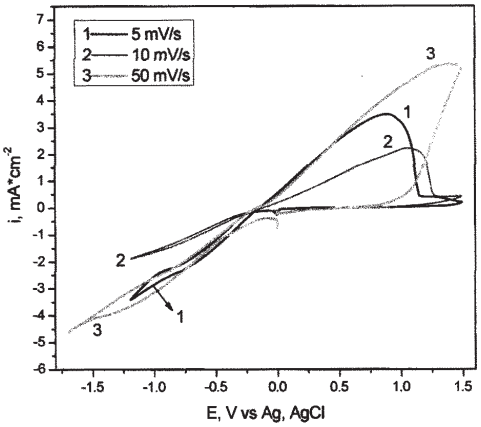

Fig. 3. Cyclic voltammograms on Pt at 25^{0}C for 50 mM $K_2[Sb_2(tartrate)_2]$ dissolved in ethylene glycol at different scan rates

Figure 3 shows a family of CV curves exhibiting deposition and dissolution processes in solution containing EG + 50 mM Sb(III) ions. The precursor was antimony potassium tartrate. It can be seen during direct scan the cathodic shoulder representing the massive deposition of antimony which is continued with supplementary cathodic processes of EG reduction and hydrogen evolution. The main reduction of Sb(III) ions has limiting current densities increasing with scan rate, suggesting also a mass-transport control. In the inverse scans, in all cases an oxidation peak with Sb stripping from Pt surface occurred in the range from +1 V to +1.4 V.

As figure 4 shows, if the Pt electrode is polarized at two different potentials, EIS diagrams for the Sb/EG system indicate semicircles with decreased Nyquist diameter and also lowering of impedance modulus and maximum phase angle (from Bode graph). Although the data is somewhat dispersed, EIS results suggest a significant deposition of antimony at -1 V potential polarization.

As a preliminary investigation of solutions containing both cobalt and antimony ions we present in figures 5 comparative voltammograms recorded in solutions with different mole ratios between Co(II) and Sb(III) ions, namely 132 mM + 25mM (fig. 5a) and 270 mM + 25 mM (fig. 5b), respectively. Of course, the shape of CV curves does not change significantly owing to predominance of

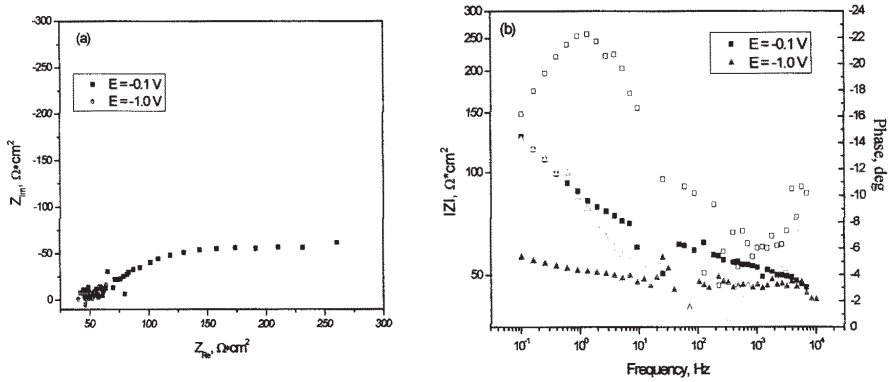

Fig. 4. Nyquist (a) and Bode (b) diagrams on Pt electrode from ethylene glycol + 50 mM $K_2[Sb_2(tartrate)_2]$, 25^{0}C, at various polarization potentials

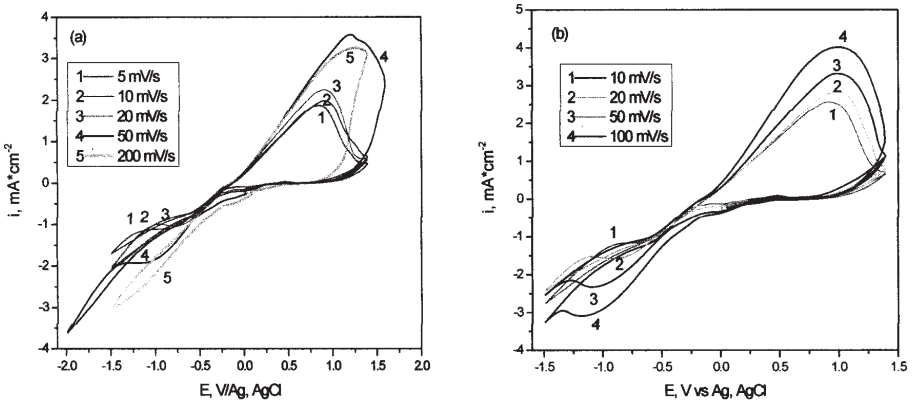

Fig. 5. Comparative CV curves on Pt at 25^{0}C for both $CoCl_2$ and $K_2[Sb_2(tartrate)_3]$ dissolved in ethylene glycol: (a) 132 mM $CoCl_2$ and 25 mM $K_2[Sb_2(tartrate)_2]$ (b) 270 mM $CoCl_2$ and 25 mM $K_2[Sb_2(tartrate)_2]$

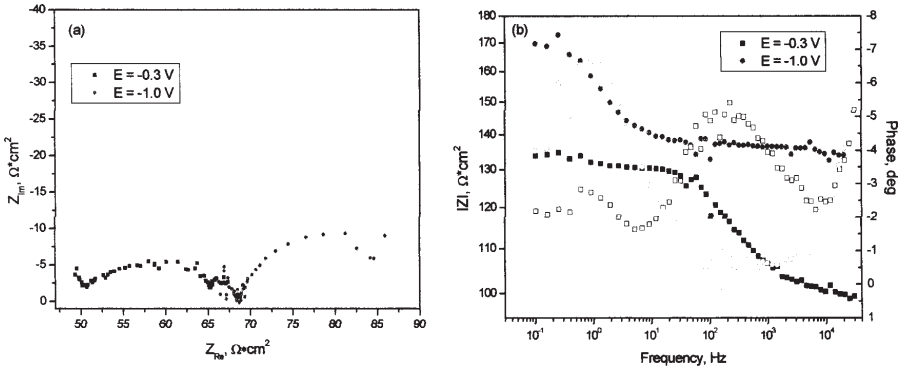

Fig. 6. Nyquist (a) and Bode (b) diagrams on Pt electrode from ethylene glycol + 50 mM $K_2[Sb_2(tartrate)_2]$, 25^{0}C, at various polarization potentials

cobalt species against antimony species. In both cases the reduction limiting currents or even cathodic peaks may be attributed to direct CoSb deposition, with a location in the potential range from -0.8 V to -1.15 V, more positively for concentrated system in cobalt ions. The dependence of currents with scan rate and Co(II) concentration suggests a mass-transport controlled process. Some differences from curves recorded with singular ions consist in more positive potentials of shoulders of peaks, as well as a crossover during inverse scan which is characteristic of a nucleation control of CoSb deposition.

EIS diagrams (fig. 6) illustrate also the particular behaviour of Co and Sb simultaneous deposition, although the data are somewhat dispersed. Thus, Nyquist loops for -0.3V and -1V polarizations have quite similar diameter value, meaning a process that begins at more positive potentials than for single Co deposition and Bode phase angle is in the same region of -5^0 or even lower.

Studies in choline chloride – ethylene glycol ionic liquid

Figure 7 shows a family of CV curves exhibiting deposition and dissolution processes in choline chloride – ethylene glycol ionic liquid containing 8 mM Co(II) ions. On the cathodic scan the massive deposition of Co takes place as the current starts to rise significantly at around -0.9 V. A new increase of current at negative potentials (more than –1.6 V) was attributed to the cathodic process of ionic liquid species, probably the reduction of choline cation. An ill-defined, rather broad electrodeposition peak is noticed, followed on the inverse scan by another broad, dissolution

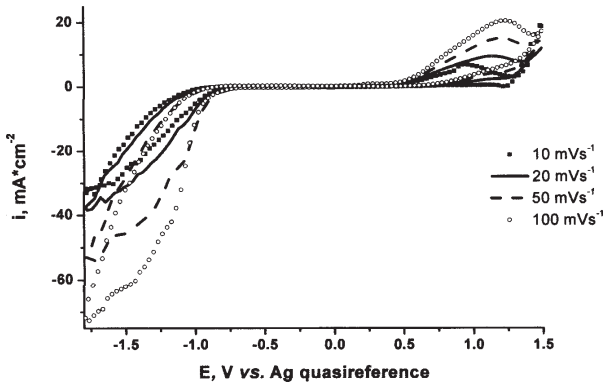

Fig. 7. Cyclic voltammograms on Pt at 60^{0}C for 8 mM $CoCl_2$ dissolved in ChCl- ethylene glycol (1:2 moles) eutectic at different scan rates

peak on the anodic branch. Both cathodic and anodic peak currents increase with scan rate, suggesting diffusion control of this quite reversible process.

The EIS spectra of ChCl–EG + $CoCl_2$ system, presented in figure 8, were obtained at different potentials of Pt electrode corresponding to the following potential domains: before metal deposition, the onset of deposition, massive deposition showing cathodic peak. From Nyquist (fig. 8a) and Bode (fig. 8b) diagrams it can be found comparatively that the plots recorded at a starting potential of -0.6 V (more positive than the onset of Co(II) ion reduction) show only a capacitive semicircle behaviour, with the highest diameter of *ca.* 1800 Ωcm^2 and the largest

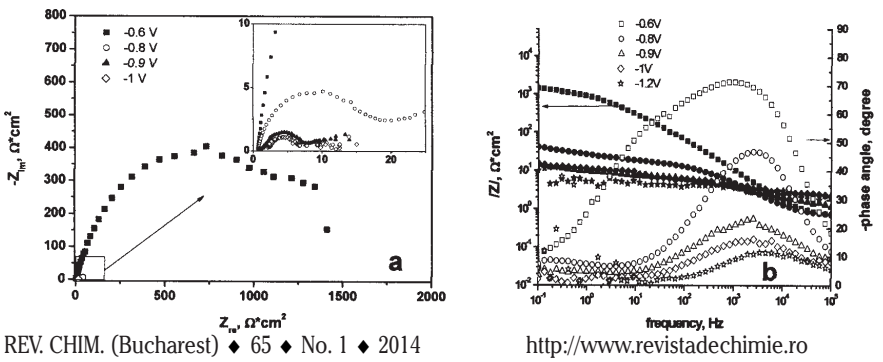

Fig. 8. Nyquist (a) and Bode (b) diagrams on Pt electrode from ChCl-ethylene glycol + 8 mM $CoCl_2$, 60^{0}C, at various polarization potentials

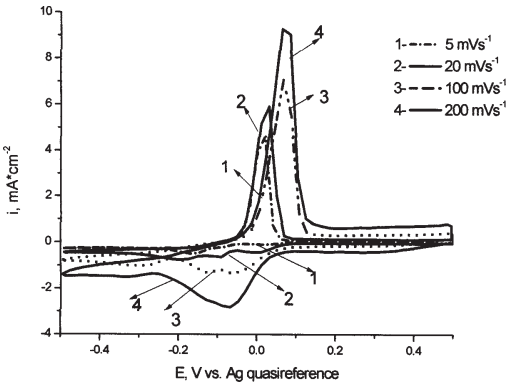

Fig. 9. Cyclic voltammograms on Pt at 60^{0}C for 9 mM $SbCl_3$ dissolved in ChCl- ethylene glycol (1:2 moles) eutectic at different scan rates

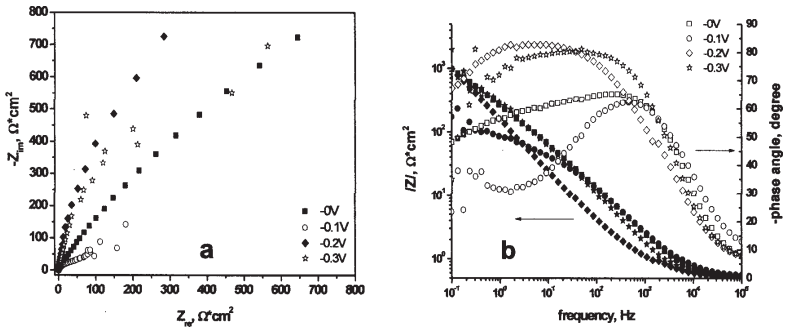

Fig. 10. Nyquist (a) and Bode (b) diagrams on Pt electrode from ChCl-ethylene glycol + 9 mM $SbCl_3$, 60^{0}C, at various polarization potentials

Bode phase angle, of -75^0. By polarizing the Pt electrode from -0.8 V to -1 V, in the range of the onset and massive deposition of metallic films, EIS spectra are similar to each other in shape, with a semicircle appearing in the high frequency domain and a straight line (a tail or a part of second semicircle) in the low frequency region. From these figures, it can be noticed that the experimental values of ohmic resistance of solution remained practically the same, of the order 1-2 Ωcm^2. The inset of figure 8a shows details of the high frequency semicircle for Co deposition; this becomes smaller in diameter, suggesting a more intensive reaction process, reaches a minimum (value of 5 Ωcm^2 at –1 V). The maximum Bode angles diminish from –50^0 (–0.8V) to –11^0 (–1.2V).

In figure 9 are presented the experimental results of cyclic voltammetry used for Pt electrode in ChCl-ethylene glycol eutectic with 9 mM $SbCl_3$ dissolved. The antimony started to deposit at +0.1V, and displayed an increasing current during the negative going scan, with a cathodic peak at 0 V ÷ -0.2 V. Only a single couple of reduction/ oxidation peaks can be seen from figure 9, the electrochemical processes being assigned to massive deposition of Sb and its film stripping from Pt electrode, respectively.

Figures 10 (a,b) show Nyquist and Bode diagrams obtained at various electrode potentials, the temperature being 60^{0}C. During the experimental procedure, the potential of the cathode was consecutively maintained at increasingly negative values: first at potentials where the reduction process does not start, then in the region of beginning the process, reaching the maximum cathodic current (-0.1 V ÷ -0.2 V) and, finally, in the region of massive metal deposition (-0.3 V). The Nyquist spectra show clearly capacitive semi-circles in the region of high frequencies. The gradually increase of the semi-circle diameter (diminution of the charge transfer resistance), if the electrode potential is more negative, indicates the decrease of electrodeposition current. The same behaviour by polarizing Pt electrode at various electrode potentials is evidenced in Bode diagrams. In figure 10b the phase angle at -0.1 V shows a single maximum around -65^0, meaning a significant capacitive behaviour. For more negative potentials, this maximum shifts toward lower frequencies and remains at high negative values of phase angle.

The cyclic voltammetric behaviour of 4 mM $CoCl_2$ + 9 mM $SbCl_3$ and 8 mM $CoCl_2$ + 4 mM $SbCl_3$ solutions in ChCl-ethylene glycol is described in figures 11. The first reduction peak (at around -0.2 V) on cathodic branch of voltammograms may be associated with antimony deposition on naked platinum surface. The second cathodic peak (in the potential region from -0.85 V to -1.1 V) may be

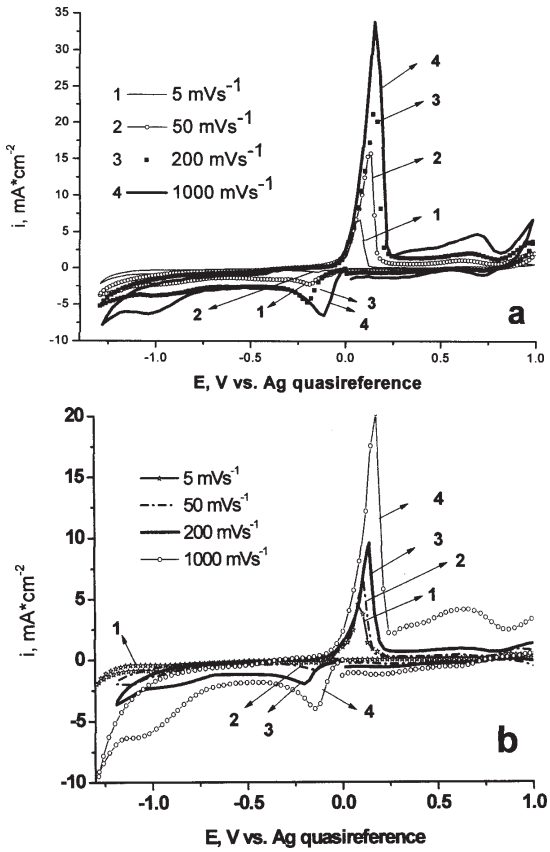

Fig. 11. Comparative CV curves on Pt at 60^{0}C for both $CoCl_2$ and $SbCl_3$ dissolved in ChCl-ethylene glycol (1:2 moles) eutectic: (a) 4 mM $CoCl_2$ and 9 mM $SbCl_3$; (b) 8 mM $CoCl_2$ and 4 mM $SbCl_3$

attributed to simultaneous deposition (co-deposition) of cobalt and antimony, with a current density much lower than cobalt deposition from solution containing single Co(II) ions (see the comparison made in fig. 12). By reverse scanning (in the anodic direction), on each voltammogram in figure 11 the first oxidation peak centered at +0.1 V ÷ +0.2 V is considered to be the preferential antimony dissolution from the deposited layers.

Further, the second anodic peak at +0.7 V is the oxidation of remaining cobalt from the cathodic deposit. A comparison between 4 mM $CoCl_2$ + 9 mM $SbCl_3$ system and 8 mM $CoCl_2$ + 4 mM $SbCl_3$ system, both represented in figures 11, indicates that the first oxidation peak has a higher value of peak current for the system with higher antimony content in electrolyte; this may be a evidence of a higher antimony content in the corresponding cathodic deposit.

EIS results obtained from the same electrolytes containing either 4 mM $CoCl_2$ + 9 mM $SbCl_3$ or 8 mM $CoCl_2$ + 4 mM $SbCl_3$, confirm the voltammetric data. Thus, the semicircle at -0.1 V in Nyquist diagrams has the shortest

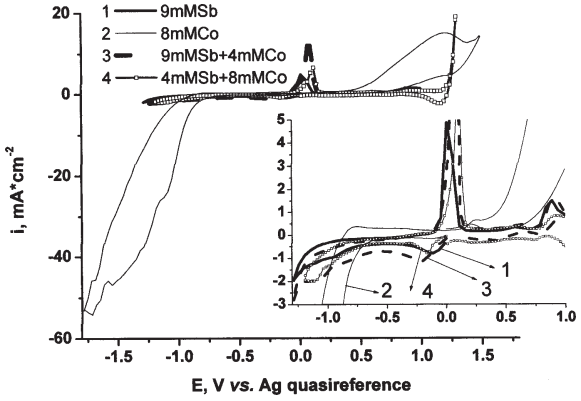

Fig. 12. Comparative CV curves on Pt at 60^{0}C for single $CoCl_2$ or $SbCl_3$ and for both $CoCl_2$ and $SbCl_3$ dissolved in ChCl-ethylene glycol (1:2 moles) eutectic; scan rate 50 mVs^{-1}

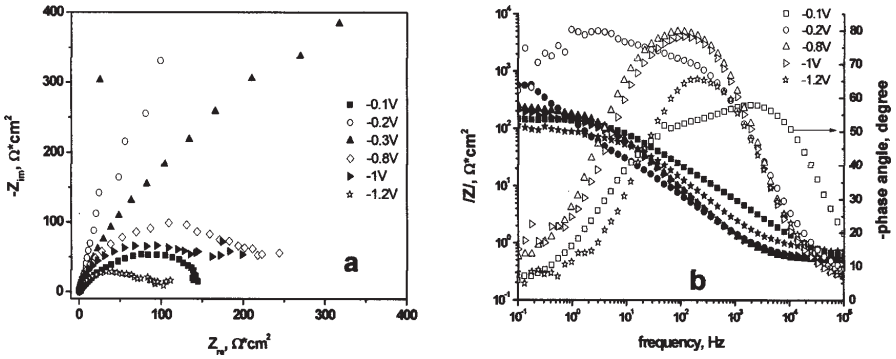

Fig. 13. Nyquist (a) and Bode (b) diagrams on Pt electrode from ChCl-ethylene glycol + 4 mM $CoCl_2$ + 9 mM $SbCl_3$, 60^{0}C, at various polarization potentials

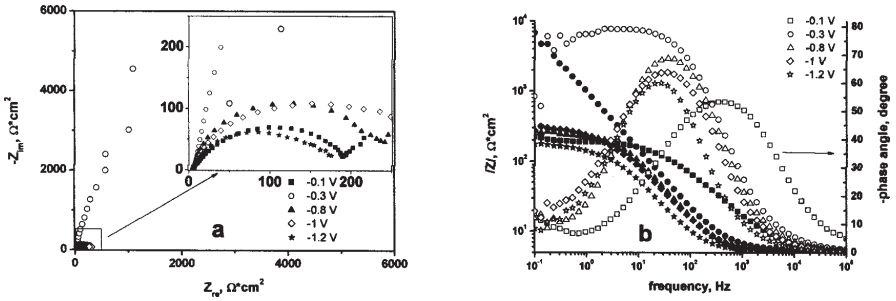

Fig. 14. Nyquist (a) and Bode (b) diagrams on Pt electrode from ChCl-ethylene glycol + 8 mM $CoCl_2$ + 4 mM $SbCl_3$, 60^{0}C, at various polarization potentials

diameter due to the beginning of antimony deposition; next, the semicircle diameter increases by more Sb layers grown on Pt electrode and then decreases by polarizing from -0.2 V to more negative potentials. Starting from -0.8 V potential the CoSb semiconductor compound is formed with gradual decrease of semicircle diameter. The maximum phase angle follows the same order.

Conclusions

The results of applying cyclic voltammetry technique evidenced a single pair of reduction/oxidation processes for each medium containing ethylene glycol and a single kind of cobalt or antimony ions. In ionic liquids with both Co and Sb ions, a first process of Sb deposition occurs before Co + Sb co-deposition. Electrochemical impedance spectra confirmed the order of cathodic processes by exhibiting the impedance behaviour (values of semicircle diameter, impedance modulus and maximum phase angle). The investigations demonstrate the possibility of CoSb deposition in both liquid media.

Acknowledgements: One of the authors recognizes financial support from the European Social Fund through POSDRU/107/1.5/S/76813 Project.

References

1. XIAO, F., HANGARTER, C., YOO, B., RHEEM, Y., LEE, K.H., MYUNG, N.V., *Electrochim. Acta,* **53**, 2008, p. 8103.
2. KLITZKE, J.P., Dissertation, University of California, Berkeley, 2009.
3. LIU, W.S., ZHANG, B.P., ZHAO, L.D., LI, J.F., Chem. Mater., **20** (24), 2008, p. 7526.
4. BALLIKAYA, C., UZAR, N., YILDIRIM, S., SALVADOR, J.R., UHER, C., 9th EUROPEAN CONF. ON THERMOELECTRICS: ECT 2011. AIP Conf. Proc., **1449**, 2012, p. 235.
5. MENDOZA-HUIZAR, L.H., RIOS-REYES, C.H., J. Solid State Electrochem., **15** (4) 2011, p. 737.
6. ZARASKA, L., KUROWSKA, E., SULKA, G.D., JASKUŁA, M., Appl. Surf. Sci. **258**, 2012, p. 9718.
7. BRYNGELSSON, H., ESKHULT, J., EDSTRÖM, K., NYHOLM, L., Electrochim. Acta, **53,** 2007, p. 1062.
8. BRYNGELSSON, H., ESKHULT, J., NYHOLM, L., HERRANEN, M., ALM, O., EDSTRÖM, K., Chem. Mater., **19**, 2007, p. 1170.
9. SADANA, Y.N., KUMAR, R., Surf. Technol., **11**, 1980, p. 37.
10. NINEVA, S., DOBROVOLSKA, T.S., KRASTEV, I., Zastita Materijala, **52**, 2011, p. 80.
11. CHENG, H., HNG, H.H., MA, J., XU, X.J., J. Mater. Res. **23**, (11), 2008, p. 3013.
12. CHENG, H., HNG, H.H., MA, J., Solid State Phenom., **136**, 2008, p. 75.
13. CUI, C.Q., JIANG, S.P., TSEUNG, A.C.C., J. Electrochem. Soc., **138,** 1991, p. 94.
14. GRZYBKOWSKI, W., PILARCZYK, M., J. Electrochem. Soc. 82, 1986, p. 1703.
15. CUI, C.Q., JIANG, S.P., TSEUNG, A.C.C., J. Electrochem. Soc., **138,** 1991, p. 1001.
16. SIMKA, W., PUSZCZYK, D., NAWRAT, G., Electrochim. Acta, **54**, (23), 2009, p. 5307.
17. CARLIN, R.T., DE LONG, H.C., FULLER, J., TRULOVE, P.C., J. Electrochem. Soc., **145,** 1998, p. 1598.
18. CHEN, P.Y., SUN, I.W., Electrochim. Acta, **46,** 2001, p. 1169.

19. FREYLAND, W., ZELL, C.A., ZEIN EL ABEDIN, S., ENDRES, F., Electrochim. Acta, **48,** (20-22), 2003, p. 3053
20. ALI, M.R., NISHIKATA, A., TSURU, T., Indian J. Chem. Technol., 12, 2005, p. 648.
21. FUKUI, R., KATAYAMA, Y., MIURA, T., Electrochim. Acta, **56**, 2011, p. 1190.
22. SCHALTIN, S., NOCKEMAN, P., THIJS, B., BINNEMANS, K., FRANSAER, J., Electrochem. Solid-State Lett. **10**, 2007, p. D104.
23. AN, M.Z., YANG, P.X., SU, C.N., NISHIKATA, A., TSURU, T., Chin. J. Chem., **26,** 2008, p. 1219.
24 YANG, P.X., AN, M.Z., SU, C.N., WANG, F.P., Electrochim. Acta, **54,** 2008, p. 763.
25 SU, C.N., AN, M.Z., YANG, P.X., GU, H., GUO, X., Appl. Surf. Sci., **256,** 2010, p. 4888.
26. YANG, M.H., SUN, I.W., J. Appl. Electrochem., **33**, 2003. p. 1077.
27. GOMEZ, E., COJOCARU, P., MAGAGNIN, L., VALLES, E., J. Electroanal. Chem., **658,** 2011, p. 18.
28. GOLGOVICI, F., COJOCARU, A., AGAPESCU, C., JIN, Y., NEDELCU, M., WANG, W., VISAN, T., Studia Univ. Babes-Bolyai, Chemia **54** (Spec. Issue 1), 2009, p. 175.
29. MARES, M.L., GOLGOVICI, F., VISAN, T., Chalcog. Lett. **10** (8), 2013, in press.
30. YAMAMOTO, H., MORISHITA, M., MIZUTA, Y., MASUBUCHI, A., Surf. Coat. Technol., **206,** 2012, p. 3415

Manuscript received: 13.08.2013